THE JOURNAL OF PHYSICAL CHEMISTRY A

Article

A High Temperature Experimental and Theoretical Study of the Unimolecular Dissociation of 1,3,5-Trioxane

Awad B. S. Alquaity, Binod Raj Giri, John M.H. Lo, and Aamir Farooq

J. Phys. Chem. A, **Just Accepted Manuscript** • DOI: 10.1021/acs.jpca.5b01801 • Publication Date (Web): 15 May 2015

A High Temperature Experimental and Theoretical Study of the Unimolecular Dissociation of 1,3,5-Trioxane

Awad B.S. Alquaity[1], Binod Raj Giri[1*], John M. H. Lo[2], Aamir Farooq[1*]

[1]Clean Combustion Research Center, Division of Physical Sciences and Engineering,

King Abdullah University of Science and Technology (KAUST), Thuwal, 23955-6900, Saudi Arabia

[2]Department of Chemistry, University of Calgary, Calgary, AB T2L 2K8, Canada

ABSTRACT

Unimolecular dissociation of 1,3,5-trioxane was investigated experimentally and theoretically over a wide range of conditions. Experiments were performed behind reflected shock waves over the temperature range of 775 – 1082 K and pressures near 900 Torr using a fast response time-of-flight mass spectrometer (TOF-MS) coupled to a shock tube (ST). Reaction products were identified directly and it was found that formaldehyde is the sole product of 1,3,5-trioxane dissociation. Reaction rate coefficients were extracted by the best fit to the experimentally measured concentration time-histories. Additionally, high-level quantum chemical and RRKM calculations were employed to study the fall off behavior of 1,3,5-trioxane dissociation. Molecular geometries and frequencies of all the species were obtained at the B3LYP/cc-pVTZ, MP2/cc-pVTZ and MP2/aug-cc-pVDZ levels of theory, whereas the single-point energies of the stationary points were calculated using coupled-cluster with single and double excitations including the perturbative treatment of triple excitation (CCSD(T)). It was found that the dissociation occurs *via* a concerted mechanism requiring to overcome an energy barrier of 48.3 kcal/mol. The new experimental data and theoretical calculations serve as a validation and extension of kinetic data published earlier by other groups. Calculated values for the pressure limiting rate coefficient can be expressed as:

$$\mathrm{Log}_{10}k_{\infty}\ (\mathrm{s}^{-1}) = [15.84 - (49.54(\mathrm{kcal/mol})/2.3RT)] \qquad (500 - 1400\ \mathrm{K})$$

INTRODUCTION

Formaldehyde (CH_2O) is an important intermediate in the combustion of hydrocarbon fuels. It is formed during the oxidation of alkanes, natural gas, alcohols, aldehydes, ethers and others.[1-3] Its importance in combustion led to a number of high temperature kinetic studies for its pyrolytic dissociation[3-6] and bimolecular reactions.[1,7-10] A substantial number of earlier studies[5,7,9, 11-16] consisted of utilizing 1,3,5-trioxane ($C_3H_6O_3$) as a clean thermolytic source of formaldehyde to avoid the problem of formaldehyde polymerization. These studies assumed reaction (1)

$$C_3H_6O_3 \rightarrow 3\ CH_2O \quad (1)$$

to be an instantaneous process at high temperatures (above 1300 K $\tau < 0.5$ μs)[5] to yield three formaldehyde molecules *via* a simple unimolecular and probably a concerted mechanism[12,17]. This mechanism for 1,3,5-trioxane decomposition was confirmed in a laser schelieren study by Irdam and Kiefer[14] and later by Aldridge et al.[12] and Hochgreb and Dryer[13].

Hogg et al.[11] and Burnett and Bell[15] measured the rate coefficients for the thermal dissociation of trioxane in a static reactor at T = 545 to 620 K and $p \leq 100$ Torr. The values of the rate coefficients reported by Hogg et al.[11] are about 40% higher than those reported by Burnett and Bell[15] at a specific temperature. Hogg et al.[11] consistently observed that the final pressure of their reactor was three times the initial pressure and concluded that the pressure rise was caused due to the dissociation of trioxane to form three formaldehyde molecules. This conclusion was later supported by the shock tube study of Irdam and Kiefer[14] who observed the dissociation of trioxane over 950 to 1270 K and 138 to 362 Torr using laser schlieren technique. Their computed density gradient profiles, in accordance with reaction (1), were found to agree very well with the experimentally measured profiles suggesting that formaldehyde is the sole product of 1,3,5-trioxane dissociation. They also reported RRKM rates and falloff based on the selected molecular parameters that were most consistent with

the experimental data.[11,14,15] Almost a year later, Aldridge et al.[12] studied reaction (1) in a static reactor over the temperature range of 523 – 603 K and pressures of 25 - 800 Torr. In addition to the experimental work, they performed RRKM calculations using the data from BAC-MP4 quantum chemical method. Their theoretical approach adequately predicted their experimental values of the rate coefficients. However, their experimental and theoretical values were found to be significantly lower than earlier studies.[11,15] In another similar study, Hochgreb and Dryer[13] measured the rate coefficients for 1,3,5-trioxane dissociation over the temperature range of 700 – 800 K in an atmospheric pressure flow reactor. Their reported values closely matched with the high pressure limiting rate coefficients predicted by RRKM calculations of Irdam and Kiefer[14] and extrapolated values of Hogg et al.[11] and Burnett and Bell[15]. However, the measured rate coefficients of Hochgreb and Dryer[13] were found to be at least a factor of two higher than the extrapolated values of Aldridge et al.[12] Based on the analysis of the reaction products, both studies[12,13] confirmed formaldehyde to be the exclusive dissociation product of 1,3,5-trioxane. In a recent study, Wang et al.[16] developed a laser absorption technique to quantitatively measure formaldehyde (CH_2O) and acetaldehyde (CH_3CHO) concentrations. The CH_2O laser diagnostic was then utilized to investigate unimolecular dissociation of 1,3,5-trioxane behind reflected shock waves over 869 to 1037 K and $p \approx 1596$ Torr. Their measured rate coefficients at high temperatures were found to overlap nicely with Irdam and Kiefer[14] data at 350 Torr which suggest that their data at these pressures are already at or close to the high pressure limit. However, their low temperature data near 900 K were lower by a factor of two than the extrapolated value of Hochgreb and Dryer.[13] Due to the existing discrepancies in literature, an additional study rendering to detailed kinetic analysis is warranted to fully ascertain the rate coefficients of the thermal dissociation of 1,3,5-trioxane.

Here, we carried out high-level quantum chemical and statistical rate theory calculations to unravel the temperature and pressure dependence of the rate coefficient for reaction (1). Additionally, we have also performed shock tube experiments to investigate the thermal unimolecular dissociation of 1,3,5-trioxane over a wide range of experimental conditions using a fast time-response time-of-flight mass spectrometer. This work provides new experimental data and state-of-the-art theoretical calculations to ascertain the rate coefficients of unimolecular decomposition of 1,3,5-trioxane.

EXPERIMENTAL SETUP

Shock Tube (ST) Facility

Thermal dissociation of 1,3,5-trioxane was investigated behind reflected shock waves in a stainless steel shock tube at temperatures ranging from 775 to 1082 K and pressures near 900 Torr. The shock tube facility has been described in detail previously.[18-20] Therefore, only a brief description is provided here. Both the driver and driven sections of the shock tube are 9 m long with an inner diameter of 14.2 cm. The length of the driver section can be varied depending on the required test time. For the experiments reported herein, a shorter (~ 3 m) driver section was used that enabled us to achieve 1.5 ms of uniform pressure (and temperature) behind reflected shock waves. (See Figure 1.) The incident shock velocity was measured using five PCB 113B26 piezoelectric pressure transducers (PZTs) that were located axially along the last 1.3 m of the driven section. The incident shock speed at the end-wall was determined by linear extrapolation of the velocity profile. One-dimensional shock-jump equations were used to calculate the conditions (temperature and pressure) behind the reflected shock wave. The uncertainty in the measured velocity was found to be ± 0.2% which translates into < 1% uncertainty in the calculated reflected shock temperature and pressure.

Mixtures containing varying concentrations of 1,3.5-trioxane, argon and neon were prepared manometrically in a 24-liter stainless steel mixing tank equipped with a magnetic stirrer. Before preparing the mixtures, the stainless steel tank was evacuated to a pressure below 10^{-5} Torr. In the current set of experiments, argon was used as an internal standard and neon was used as a bath gas due to the comparatively high electron-impact ionization cross-sections of argon. Homogenous mixtures were prepared by mixing gases in the magnetically-stirred mixing tank. The purity of chemicals and gases used were: 1,3,5 trioxane (Sigma Aldrich, ≥99%, degassed several times before use), argon (99.9999%, AHG) and neon (99.999%, AHG).

***Time-of-Flight Mass Spectrometer* (*TOF-MS*)**

The coupling of shock tube (ST) with time-of-flight mass spectrometer (TOF-MS) for high temperature kinetic studies is a challenging task. These challenges and successful operation of ST/TOF-MS have been amicably discussed in early studies by Moulton[21,22], Bradley and Kistiakowsky[23], Krizancic et al.[24], Voldner and Trass[25] and recently by Tranter et al.[26] and Dürrstein et al.[27] Our coupling and configuration for the ST/TOF-MS is similar to the existing facilities in Karlsurhe[28,29] and Duisberg-Essen[27,30]. For kinetics studies, the samples behind the reflected shock waves are drawn continually through a conical nozzle (inner opening angle of 120^{o}) of precise pin hole size of 75 μm (±10%, Frey GmbH, Germany) centered in the end-wall of the driven section of the shock tube. The choice for the size of the nozzle is dictated by the need of keeping the ion source pressure of TOF-MS as low as possible (≤ 10^{-5} Torr) to avoid any damage to the ion source while operating the shock tube at pressures between 500 and 2250 Torr. The tip of the conical nozzle protrudes about 1 mm into the shock tube that ensures molecular beam sampling from the core shock-heated zone. This avoids the contamination of the sample by the cold thermal boundary layer that

grows to the shock heated zone following the reflection of the shock wave. A detailed discussion on the growth of the thermal boundary layer and its effect pertinent to the kinetic studies using ST/TOF-MS can be found elsewhere.[21, 25, 26] For our operating conditions, the molecular beam exiting the nozzle undergoes rapid quenching in less than 1 μs and only a small portion of the beam reaches the ion source of the TOF-MS (Stefan Kaesdorf Inc., Munich). In these studies, direct sampling from the nozzle is employed without using a skimmer. We did not employ nozzle-skimmer sampling system for three reasons: (i) the nozzle-skimmer sampling system skims off most of the molecular beam that consequently diminishes the signal intensity significantly; (ii) this arrangement requires differentially pumped molecular beam sampling interface. In our current setup, both the ion source and flight tube of TOF-MS can be pumped down to $\leq 10^{-7}$ Torr, and a pressure below 10^{-3} Torr cannot be achieved in the skimmer section of the interface due to its compactness. The inability to create a high vacuum in the skimmer section will result in inadequate quenching of the molecular beam. A rapid quenching of the representative sample from the shock heated zone via a supersonic jet expansion is very crucial in these kinds of experiments. (iii) Precise alignment of the skimmer with respect to the nozzle is critical. This alignment is challenging to achieve. A little misalignment by few degrees may lead to the ionization of the molecular beam that has originated from the vicinity of the shock tube wall and hence may have been affected by the cold thermal boundary layer.

For a successful operation of ST/TOF-MS system, the separation distance between the sampling orifice and ionization location plays a crucial role. In the original design, this separation was 42.75 mm. To increase the sensitivity, we modified our coupling to reduce this separation to 35.75 mm. As the molecular beam reaches the ionization zone of the ion source, it is bombarded with electrons to produce ions. Our TOF-MS employs a two-stage ion extraction for space-focusing that compensates the ions starting from different locations of

the ionization zone. The experiments reported here used optimum ionization energy of 34 eV that greatly suppressed the ionization of the bath gas (neon). It entails an important aspect of the experiment to avoid saturation of the micro-channel plate (MCP, Photonics Inc., USA, type E25-10-D-SET) detector. The TOF-MS can be operated up to a maximum repetition rate of 150 kHz (6.7 μs), however, in this study, a repetition rate of 100 kHz (10 μs) was employed. The reduced repetition rate helps to avoid saturation of the MCP detector and any intermingling of the ions from successive ionization events. The MCP signal is amplified using a pre-amplifier that enables us to use the lowest possible voltage supply to the MCP, thus avoiding saturation of the detector. This is crucial when TOF-MS is operated at the high repetition rates ≥ 100 kHz. To avoid any possible arching of the ion source due to sudden rise in pressure, the TOF-MS is automatically shut down after 1 second using an interlock system. The analog signal from MCP detector was recorded using an 8-bit digitizer (Agilent U1071A) at a sampling rate of 1 GHz for a total recording time of 2.5 ms. For each shock wave experiment, the recorded data contains about 500 μs of pre-shock data and the remaining 2 ms of post-shock data. The recorded data, representing mass spectra for a total of 2500 ionization events, were de-convoluted into sub-packets (containing mass spectra for each ionization event) using an in-house Matlab code. The time-histories for the species of interest were obtained by integrating the peaks from successive ionization events.

QUANTUM CHEMICAL CALCULATIONS

The structures of the stationary points along the reaction pathway for the unimolecular dissociation of trioxane were optimized by using the density functional theory with the hybrid Becke-3-Lee-Yang-Parr (B3LYP) functional[31-33] using all-electron Dunning's correlation-consistent polarized valence triple zeta basis sets (cc-pVTZ) for C, H, O.[34,35] In addition, geometry optimizations were also carried out at the second order Møller-Plesset (MP2)[36,37]

perturbation theory using Dunning's augmented correlation-consistent double zeta basis set (aug-cc-pVDZ)[34,38]. These optimized structures were further characterized by normal mode analysis to confirm their identities on the potential energy surfaces. The computed vibrational frequencies at the B3LYP/cc-pVTZ and MP2/aug-cc-pVDZ levels of theory were scaled by 0.9615 and 0.9682, respectively.[32]

Based on the optimized geometries, single-point coupled-cluster calculations with single and double excitations[39-42], including the perturbative treatment of triple excitation (CCSD(T))[26], were carried out for the energetic description of minimum structures and transition states. Several Dunning's correlation-consistent polarized valence cc-pV*X*Z (*X* = D, T, and Q) basis sets[27,28] were used to extrapolate to the complete basis set (CBS) limit. We employed the extrapolation scheme developed by Helgaker et al.[29,30] Here, we treated the Hartee-Fock and correlation energies separately. The Hartee-Fock energy at the infinite basis set limit ($E_{\infty,\mathrm{HF}}$) was obtained through extrapolation, according to $E_{\mathrm{HF}}(X) = E_{\infty,\mathrm{HF}} + b^{*}\exp(-cX)$ with Dunning's correlation-consistent polarized valence X = 2 (double), 3 (triple), and 4 (quadruple) zeta basis sets[31]. For the correlation energy, we used $E_{\mathrm{corr}}(X) = E_{\infty,\mathrm{corr}} + b'X^{-3}$ with X = 2 and 3 for cc-pVDZ and cc-pVTZ basis sets, respectively.[29] All calculations were performed using the Gaussian 09 package.[43]

RRKM theory[44-46] was employed to calculate the pressure- and temperature- dependence of the rate coefficients for the unimolecular dissociation of trioxane using the data from quantum chemical calculations. For these calculations, the program script developed by Kiefer et al.[47,48] was used.

RESULTS AND DISCUSSION

Figure 2 shows a sample profile for the raw data obtained from our ST/TOF-MS experiment. Here, the downward spikes are the signal intensities of various species and the

upward spikes are the timing signal. A single 10 μs time segment taken from the post-shock condition (1.4 ms after the arrival of reflected shock; T_5 = 1082 K and p_5 = 1.2 bar) is displayed in Fig. 3 where all peaks are identified. In Fig. 3, the rising part of the timing signal is the start of ionization, whereas the falling part indicates the injection of ion packets for that particular ionization event. The time window between the falling and the rising parts of the timing signal corresponds to the duration of ionization. In these experiments, the ionization duration was set to 1 μs. In our measurements, the reaction progress was monitored simultaneously for the reactant, 1,3,5-trioxane ($C_3H_6O_3$), and the product, formaldehyde (H_2CO). As can be seen, the reactant observed at m/z = 31 for H_3CO^+ (a strong fragment of trioxane as the parent ion is not observed) has reacted away completely at this relatively late reaction time (1.4 ms). Clearly, an ionization interval of 10 μs is long enough to accommodate all ions that appear in a given ionization event without intermingling of ions from successive events. The m/z ratio for each peak appearing in the mass spectrum is determined using the relationship, $m/z = a(t_f)^2 + b(t_f) + c$; where t_f is the time-of-flight of the ions, *a, b and c* are constants determined via calibration. Apart from Ar (m/z = 40) and Ne (m/z = 20), the remaining peaks (m/z = 30, 29 and 28) correspond to formaldehyde (m/z = 30) and its fragments CHO^+ (m/z = 29) and CO^+ (m/z = 28). This clearly indicates that formaldehyde is the sole product of 1,3,5-trioxane dissociation. The experiments carried out in the current work thus provide further evidence that formaldehyde is the only product of 1,3,5-trioxane dissociation.

The peaks of interest from each ionization event were integrated using an in-house Matlab code to generate peak area versus time profiles. The area of each peak is scaled by the peak area of the internal standard. Here, we used argon (Ar) as internal standard to correct any variations in the sensitivity of TOF-MS. Absolute concentration-time-profiles for trioxane and formaldehyde were obtained from calibration experiments using the relationship

$\frac{I_x}{I_{Ar}} = m \frac{p_x}{p_{Ar}}$, where m is the calibration factor; I and p are the ion intensity and partial pressure of the species (x), respectively. The calibration curves are given in Fig. IS of the Supporting Information. The calibration experiments were performed near 900 Torr and about 600 K for trioxane and about 1200 K for formadehyde. Near 600 K, trioxane does not dissociate within the time scale of our experiments. Similarly at about 1200 K of our ST/TOF-MS experiments, a constant concentration-time-profile for formaldehyde is achieved via instantaneous dissociation of trioxane. For the calibration experiments, the partial pressure of trioxane was varied by keeping argon (internal standard) concentration constant. A typical plot for the concentration-time-profiles of 1,3,5-trioxane and formaldehyde is shown in Fig. 4. An additional representative case is shown in Fig. IIS of the Supporting Information.

For reaction (1), potential energy surface was mapped out at the CCSD(T)/cc-pVTZ//B3LYP/cc-pVTZ and CCSD(T)/CBS//MP2/aug-cc-pVDZ levels of theory. At B3LYP/cc-pVTZ optimized geometry, the calculated barrier height (E_0) for the unimolecular dissociation of 1,3,5-trioxane comes out to be 48.62 kcal/mol at the CCSD(T)/cc-pVTZ level of theory, whereas a barrier height of 48.30 kcal/mol was computed at the CCSD(T)/CBS//MP2/aug-cc-pVDZ level of theory. Our CCSD(T)/CBS value of 49.2 kcal/mol at 298 K was found to be in very good agreement with that reported by Aldridge et al.[12] (49.1 kcal/mol at 298 K) who used the bond additivity correction method at the level of fourth-order Møller-Plesset perturbation theory (BAC-MP4). We performed T_1 diagnostic of Lee et al.[49,50] to assess the multi-reference character of the wave function. For our stationary points, all values for T_1 were found to be smaller than 0.02 implying that single-reference method is appropriate. Our optimized geometry at the MP2/aug-cc-pVDZ level of theory reveals that the most stable form of 1,3,4-trioxane occurs in the chair form with C-O bond length of 1.4198 Å. In the transition state (TS), the three C-O dissociating bonds stretch to 1.9307 Å, whereas the remaining three C-O bonds shorten to 1.2632 Å, which is very close to

that of the product ($r_{C\text{-}O}$ = 1.2237 Å in formaldehyde). As noted earlier, the reaction step 1,3,5-trioxane → TS requires to overcome a barrier of about 48 kJ/mole at the CCSD(T) level of theory. The low value for the activation energy (≈50 kcal/mole) observed in the experiments agrees well with our computed barrier height for reaction (1) which clearly infers that 1,3,5-trioxane dissociation occurs via a concerted mechanism. Furthermore, our calculations performed at the CCSD(T)/CBS level of theory predict that the unimolecular dissociation of trioxane is an endothermic process ($\Delta_r H°$ = 30.3 and 33.82 kcal/mol at 0 and 298 K, respectively). Combining this value of heat of reaction with the heat of formation of formaldehyde ($\Delta_f H^\circ$ = -25.06 and -25.97 kcal/mol at T = 0 and 298 K, respectively), the enthalpy of formation ($\Delta_f H^\circ$(g)) of trioxane is calculated to be -105.5 and -111.8 kcal/mol at 0 and 298 K, respectively. Our calculated value ($\Delta_f H^\circ$(g) = -105.5 kcal/mol) matches very well to that reported by Aldridge et al.[12] ($\Delta_f H^\circ$(g) = -104.28 kcal/mol) using the BAC-MP4 method within the uncertainty[51] of BAC-MP4 method. Also, our calculated value is found to be in good agreement with that found from the heat of combustion of 1,3,5 trioxane ($\Delta_f H^\circ$(g) = -110.7 kcal/mol)[52] and with the value (-116±5 kcal/mol) used by Irdam and Kiefer[14] to model their experimental density gradient profiles. To account for non-isothermal effects arising from the endothermicity of the reaction ($\Delta_r H°$ = 33.82 kcal/mol at 298 K), chemical kinetic simulations comprising of only reaction (1) were performed to extract the initial rate coefficients. For kinetic simulation, we started with an initial estimate of the rate constant from Irdam and Kiefer[14] and varied iteratively to obtain the best fit with the measured concentration time-profiles. An example of such kinetic simulations is shown in Fig. 4 (solid lines). (See also in Figure IIS). The extracted rate coefficients from all our experiments are listed in Table 1 and plotted with the literature data in Fig. 5. As can be seen, our data fill up the void spaces in the mid-temperature range and encompass both the Irdam and Kiefer[14] and Wang et al.[16] data at high temperatures. Our values of the rate coefficients (±30%) measured

near 900 Torr compare very well with that reported by Irdam and Kiefer[14] and Wang et al.[16] (±20%) at pressures of 350 and 1596 Torr, respectively. This indicates that the measured rates over 350 – 1596 Torr are quite close to the high-pressure limit. As we expect to see little or no pressure dependence for reaction (1) at low temperatures. our rate coefficients at the lower temperature end show an excellent agreement with the data from Hochgreb et al.[13] and also with the extrapolated value of the low pressure and low temperature data from Hogg et al. [11] and Burnett and Bell[15].

Our experimental data were further rationalized in terms of RRKM calculations using the data from ab-initio calculations. Based on the parameters compiled in Table 2, we computed pressure- and temperature- dependent rate coefficients for reaction (1) using Kiefer et al.[47,48] RRKM program script. As can be seen in Fig. 5, our calculated RRKM rates match very well with the available experimental data at all temperatures and pressures with an average absolute deviation of 16.5%. The low temperature data of Aldridge et al.[12] appear to be too slow and are not captured by our calculations. Excluding the data from Aldridge et al.[12], the calculated rate coefficients ($k(T, p)$) were found to be most consistent with the available data for a barrier height (E_0) of 46.5 kcal/mol. To achieve the agreement between theory and experiments, such as the one shown in Figure 4, the calculated threshold energy was adjusted by about 1.8 kcal/mol. This adjustment of the barrier height is reasonable considering the uncertainties associated with these ab-initio calculations. Furthermore, we note that the RRKM results reported here are for neon as bath gas while Irdam and Kiefer[14] used krypton and Wang et al.[16] used argon as bath gas in their experiments. However, the bath gas is expected to cause negligible change in the calculated values of the rate coefficient. The parameters for the calculated values of the pressure dependent rate coefficient are compiled in Table 3 over the temperature range of 500 to 1400 K.

CONCLUSIONS

Thermal unimolecular dissociation of 1,3,5-trioxane was investigated behind reflected shock waves over 775 K – 1082 K and pressures near 900 Torr. Reaction progress was monitored using time-of-flight mass spectrometer as a diagnostic tool. It was found that formaldehyde is the sole product of 1,3,5 trioxane dissociation. To analyze our kinetic results, coupled cluster calculations were performed to explore the potential energy surface for 1,3,5-trioxane dissociation. It was found that the dissociation occurs *via* a concerted mechanism requiring to overcome an energy barrier of *ca.* 48 kcal/mole at the CCSD(T)/CBS//MP2/aug-cc-pVTZ level of theory. This value of the threshold energy matches very well to that found by the best fit of the experimental data to the RRKM model. A small adjustment of the barrier height by about 1.8 kcal/mol resulted in an excellent agreement between the theoretical and available experimental rate coefficients at all pressures and temperatures.

ACKNOWLEDGEMENTS

Research reported in this publication was funded by King Abdullah University of Science and Technology (KAUST). Experimental work was carried out at the Chemical Kinetics and Laser Sensors Laboratory at KAUST. The computations described in this work were performed using the computing facilities of the department of Academic Information and Communication Technologies (AICT) and the High-Performance Computing (HPC) facilities of the University of Calgary, the Western Canada Research Grid and the computing facility at the University of Szeged, Hungary. The authors would like to thank Dr. Milan Szőri (University of Szeged, Hungary) for invaluable discussions.

ASSOCIATED CONTENT

Supporting Information

Rotational constants and harmonic wavenumbers of all species obtained using various levels of theory are provided in the Supporting Information (Tables IS, IIS and IIIS). Calibration curves and representative data are provided in Figs. IS and IIS, respectively. This material is available free of charge via the Internet at http://pubs.acs.org.

AUTHOR INFORMATION

Corresponding Author

*E-mail: binod.giri@kaust.edu.sa; Phone:+966544700873

aamir.farooq@kaust.edu.sa; Phone:+966544700621

Notes

The authors declare no competing financial interest.

REFERENCES

1. Choudhury, T. K.; Lin, M. C., Pyrolysis of Methyl Nitrite and 1,3,5-Trioxane Mixtures in Shock Waves: Kinetic Modeling of the H + CH_2O Reaction Rate. *Combust. Sci. Technol.* **1989,** *64* (1-3), 19-28.
2. Westbrook, C. K.; Dryer, F. L., Comprehensive Mechanism for Methanol Oxidation. *Combust. Sci. Technol.* **1979,** *20* (3-4), 125-140.
3. Peeters, J.; Mahnen, G., Reaction Mechanisms and Rate Constants of Elementary Steps in Methane-Oxygen Flames. *Symp. (Int.) Combust.* **1973,** *14* (1), 133-146.
4. Gay, I. D.; Glass, G. P.; Kistiakowsky, G. B.; Niki, H., Pyrolysis and Oxidation of Formaldehyde in Shock Waves. *J. Chem. Phys.* **1965,** *43* (11), 4017-4022.
5. Irdam, E. A.; Kiefer, J. H.; Harding, L. B.; Wagner, A. F., The Formaldehyde Decomposition Chain Mechanism. *Int. J. Chem. Kinet.* **1993,** *25* (4), 285-303.
6. Friedrichs, G.; Davidson, D. F.; Hanson, R. K., Validation of a Thermal Decomposition Mechanism of Formaldehyde by Detection of CH_2O and HCO Behind Shock Waves. *Int. J. Chem. Kinet.* **2004,** *36* (3), 157-169.
7. Vasudevan, V.; Davidson, D. F.; Hanson, R. K.; Bowman, C. T.; Golden, D. M., High-Temperature Measurements of the Rates of the Reactions CH_2O + Ar → Products and CH_2O + O_2 → Products. *Proc. Combust. Inst.* **2007,** *31* (1), 175-183.
8. Li, H.-Y.; Pu, M.; Ji, Y.-Q.; Xu, Z.-F.; Feng, W.-L., Theoretical Study On the Reaction Path and Rate Constants of the Hydrogen Atom Abstraction Reaction of CH_2O With CH_3/OH. *Chem. Phys.* **2004,** *307* (1), 35-43.
9. Wang, S.; Dames, E. E.; Davidson, D. F.; Hanson, R. K., Reaction Rate Constant of CH_2O + H = HCO + H2 Revisited: A Combined Study of Direct Shock Tube Measurement and Transition State Theory Calculation. *J. Phys. Chem. A* **2014,** *118* (44), 10201-10209.
10. Friedrichs, G.; Davidson, D. F.; Hanson, R. K., Direct Measurements of the Reaction H + CH_2O → H_2 + HCO Behind Shock Waves by Means of Vis − UV Detection of Formaldehyde. *Int. J. Chem. Kinet.* **2002,** *34* (6), 374-386.
11. Hogg, W.; McKinnon, D. M.; Trotman-Dickenson, A. F.; Verbeke, The Pyrolysis of 1,3,5-Trioxan, Notes. *J. Chem. Soc. (Resumed)* **1961,** (0), 1400-1420.
12. Aldridge, H. K.; Liu, X.; Lin, M. C.; Melius, C. F., Thermal Unimolecular Decomposition of 1,3,5-Trioxane: Comparison of Theory and Experiment. *Int. J. Chem. Kinet.* **1991,** *23* (10), 947-956.
13. Hochgreb, S.; Dryer, F. L., Decomposition of 1,3,5-trioxane at 700-800 K. *J. Phys. Chem.* **1992,** *96* (1), 295-297.
14. Irdam, E.; Kiefer, J., The Decomposition of 1, 3, 5-trioxane at Very High Temperatures. *Chem. Phys. Lett.* **1990,** *166* (5), 491-494.
15. Burnett, R. l. G.; Bell, R. P., The Decomposition of Gaseous Trioxymethylene and Paraldehyde. *Trans. Faraday Soc.* **1938,** *34* (0), 420-426.
16. Wang, S.; Davidson, D. F.; Hanson, R. K., High-Temperature Laser Absorption Diagnostics for CH_2O and CH_3CHO and Their Application to Shock Tube Kinetic Studies. *Combust. Flame* **2013,** *160* (10), 1930-1938.
17. Benson, S. W.; O'Neal, H. E., Kinetic Data on Gas Phase Unimolecular Reactions. 1970 ed.; National Bureau of Standards: 1970; Vol. 21, p 314.
18. Badra, J.; Khaled, F.; Giri, B. R.; Farooq, A., A Shock Tube Study of the Branching Ratios of Propene + OH Reaction. *Phys. Chem. Chem. Phys.* **2014**.
19. Badra, J.; Elwardany, A.; Farooq, A., Shock Tube Measurements of the Rate Constants for Seven Large Alkanes + OH. *Proc. Combust. Inst.* **2015,** *35* (1), 189-196;
20. Badra, J.; Nasir, E. F.; Farooq, A., Site-Specific Rate Constant Measurements for Primary and Secondary H- and D-Abstraction by OH Radicals: Propane and n-Butane. *J. Phys. Chem. A* **2014,** *118* (26), 4652-4660.
21. Moulton, D. M. Shock Wave Studies by Time of Flight Mass Spectrometry. Harvard University, Cambridge, 1964.
22. Dove, J. E.; Moulton, D. M., *Shock Wave Studies by Mass Spectrometry. III. Description of Apparatus; Data on the Oxidation of Acetylene and of Methane*. 1965; Vol. 283, p 216-228.
23. Bradley, J. N.; Kistiakowsky, G. B., Shock Wave Studies by Mass Spectrometry. I. Thermal Decomposition of Nitrous Oxide. *J. Chem. Phys.* **1961,** *35* (1), 256-263.
24. Krizancic, I.; Haluk, M.; Cho, S. H.; Trass, O., Shock Tube Coupled to the Time-of-Flight Mass Spectrometer Via a Molecular Beam Sampling System. *Rev. Sci. Instrum.* **1979,** *50* (7), 909-915.
25. Voldner, E. C.; Trass, O., Evaluation of Thermal Boundary Layer Interaction in Shock Tube Sampling for Kinetic Studies. *J. Chem. Phys.* **1980,** *73* (4), 1601-1611.

26. Tranter, R. S.; Giri, B. R.; Kiefer, J. H., Shock Tube/Time-of-Flight Mass Spectrometer for High Temperature Kinetic Studies. *Rev. Sci. Instrum.* **2007,** *78* (3), 034101.
27. Dürrstein, S. H.; Aghsaee, M.; Jerig, L.; Fikri, M.; Schulz, C., A Shock Tube With a High-Repetition-Rate Time-of-Flight Mass Spectrometer for Investigations of Complex Reaction Systems. *Rev. Sci. Instrum.* **2011,** *82* (8), 084103.
28. Dürrstein, S. H.; Olzmann, M.; Aguilera-Iparraguirre, J.; Barthel, R.; Klopper, W., The Phenyl + Phenyl Reaction as Pathway to Benzynes: An Experimental and Theoretical Study. *Chem. Phys. Lett.* **2011,** *513* (1–3), 20-26.
29. Kiecherer, J.; Bänsch, C.; Bentz, T.; Olzmann, M., Pyrolysis of Ethanol: A Shock-Tube/TOF-MS and Modeling Study. *Proc. Combust. Inst.* **2015,** *35* (1), 465-472.
30. Aghsaee, M.; Bohm, H.; Durrstein, S. H.; Fikri, M.; Schulz, C., Experimental and Modeling Study of Carbon Suboxide Decomposition Behind Reflected Shock Waves. *Phys. Chem. Chem. Phys.* **2012,** *14* (3), 1246-1252.
31. Becke, A. D., Density-functional thermochemistry. II. The Effect of the Perdew-Wang Generalized-Gradient Correlation Correction. *J. Chem. Phys.* **1992,** *97* (12), 9173-9177.
32. Becke, A. D., Density-Functional Thermochemistry. III. The Role of Exact Exchange. *J. Chem. Phys.* **1993,** *98* (7), 5648-5652.
33. Lee, C.; Yang, W.; Parr, R. G., Development of the Colle-Salvetti Correlation-Energy Formula into a Functional of the Electron Density. *Phys. Rev. B* **1988,** *37* (2), 785-789.
34. Dunning, T. H., Gaussian Basis Sets for Use in Correlated Molecular Calculations. I. The Atoms Boron Through Neon And Hydrogen. *J. Chem. Phys.* **1989,** *90* (2), 1007-1023.
35. Wilson, A. K.; Woon, D. E.; Peterson, K. A.; Dunning, T. H., Gaussian Basis Sets for Use in Correlated Molecular Calculations. IX. The Atoms Gallium Through Krypton. *J. Chem. Phys.* **1999,** *110* (16), 7667-7676.
36. Moller, C., and Plesset, M. S.}, Note on an Approximation Treatment for Many-Electron Systems. *Phys. Rev.* **1934,** *46* (7), 618--622.
37. Wiberg, K. B., Ab Initio Molecular Orbital Theory by W. J. Hehre, L. Radom, P. v. R. Schleyer, and J. A. Pople, John Wiley, New York, 548pp. Price: $79.95 (1986). *J. Comput. Chem.* **1986,** *7* (3), 379-379.
38. Kendall, R. A.; Dunning, T. H.; Harrison, R. J., Electron Affinities of the First-Row Atoms Revisited. Systematic Basis Sets And Wave Functions. *J. Chem. Phys.* **1992,** *96* (9), 6796-6806.
39. Čížek, J., On the Use of the Cluster Expansion and the Technique of Diagrams in Calculations of Correlation Effects in Atoms and Molecules. In *Adv. Chem. Phys.*, John Wiley & Sons, Inc.: 2007; pp 35-89.
40. Purvis, G. D.; Bartlett, R. J., A Full Coupled-Cluster Singles and Doubles Model: The Inclusion of Disconnected Triples.*J. Chem. Phys.* **1982,** *76* (4), 1910-1918.
41. Scuseria, G. E.; Janssen, C. L.; Schaefer, H. F., An Efficient Reformulation of the Closed-Shell Coupled Cluster Single and Double Excitation (CCSD) Equations. *J. Chem. Phys.* **1988,** *89* (12), 7382-7387.
42. Scuseria, G. E.; Schaefer, H. F., Is Coupled Cluster Singles And Doubles (CCSD) More Computationally Intensive Than Quadratic Configuration Interaction (QCISD)? *J. Chem. Phys.* **1989,** *90* (7), 3700-3703.
43. Frisch, M. J. T., G. W.; Schlegel, H. B.; Scuseria, G. E.; Robb, M. A.; Cheeseman, J. R.; Scalmani, G.; Barone, V.; Mennucci, B.; Petersson, G. A.; Nakatsuji, H.; et al. *Gaussian 09, Revision A.02*, Gaussian Inc.: Wallingford CT, 2009.
44. Gilbert, R. G.; Smith, S. C., *Theory of Unimolecular and Recombination Reactions*. Blackwell Scientific Publications: 1990.
45. Marcus, R. A., Unimolecular Dissociations and Free Radical Recombination Reactions. *J. Chem. Phys.* **1952,** *20* (3), 359-364.
46. Marcus, R. A.; Rice, O. K., The Kinetics of the Recombination of Methyl Radicals and Iodine Atoms. *J. Phys. Chem.* **1951,** *55* (6), 894-908.
47. Kiefer, J. H.; Shah, J. N., Unimolecular Dissociation of Cyclohexene at Extremely High Temperatures: Behavior of the Energy-Transfer Collision Efficiency. *J. Phys. Chem.* **1987,** *91* (11), 3024-3030.
48. Kiefer, J. H.; Mizerka, L. J.; Patel, M. R.; Wei, H. C., A Shock Tube Investigation of Major Pathways in the High-Temperature Pyrolysis of Benzene. *J. Phys. Chem.* **1985,** *89* (10), 2013-2019.
49. Lee, T. J.; Rendell, A. P.; Taylor, P. R., Comparison of the Quadratic Configuration Interaction and Coupled-Cluster Approaches to Electron Correlation Including the Effect of Triple Excitations. *J. Phys. Chem.* **1990,** *94* (14), 5463-5468.
50. Lee, T. J.; Taylor, P. R., A Diagnostic for Determining the Quality of Single-Reference Electron Correlation Methods. *Int. J. Quant. Chem.* **1989,** *36* (S23), 199-207.
51. Allendorf, M. D.; Melius, C. F., BAC-MP4 Predictions of Thermochemistry for Gas-Phase Compounds in the Si−H−O−Cl System. *J. Phys. Chem. A* **2002,** *106* (26), 6370-6380.

52. Berlin, A. A.; Vol'fson, S. A.; Oleinik, E. F.; Yenikolopyan, N. S., Thermodynamics of the Formaldehyde-Trioxane-Polyformaldehyde Equilibrium System. *Polym. Sci. U.S.S.R.* **1970,** *12* (2), 506-513.

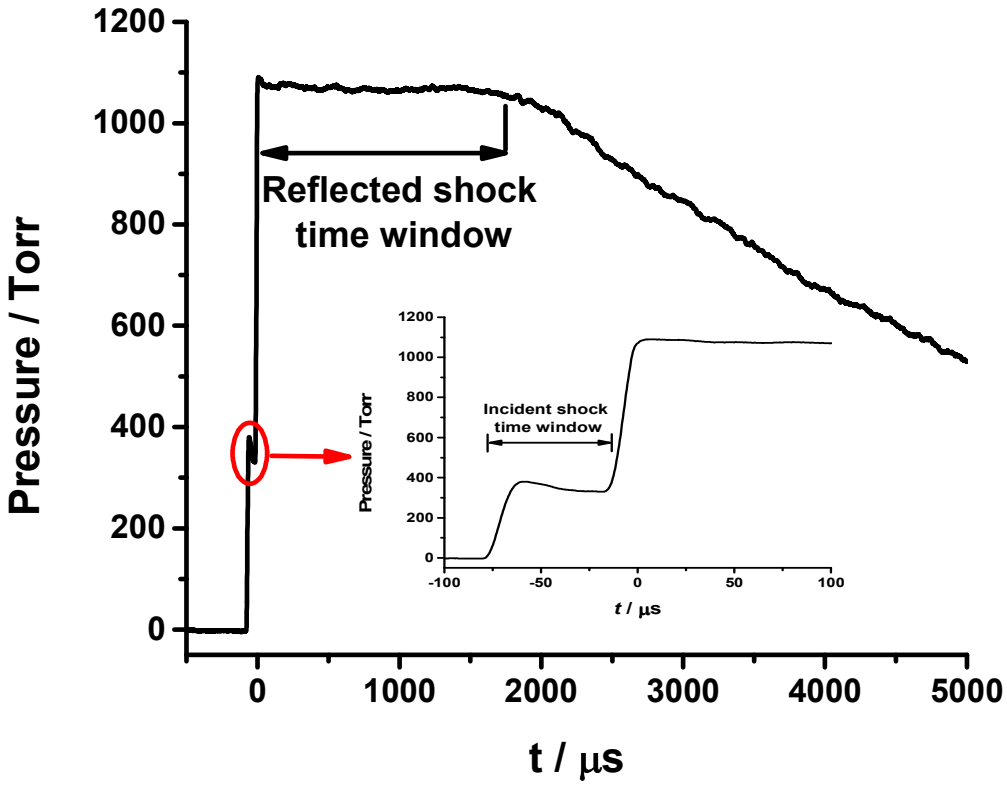

Figure 1: Representative pressure trace showing the incident and reflected shock time windows. The experimental conditions are p_5 = 1065 Torr, T_5 = 910 K, mixture composition of 2.69% Ar/ 1.2% $C_3H_6O_3$/ 96.11% Ne.

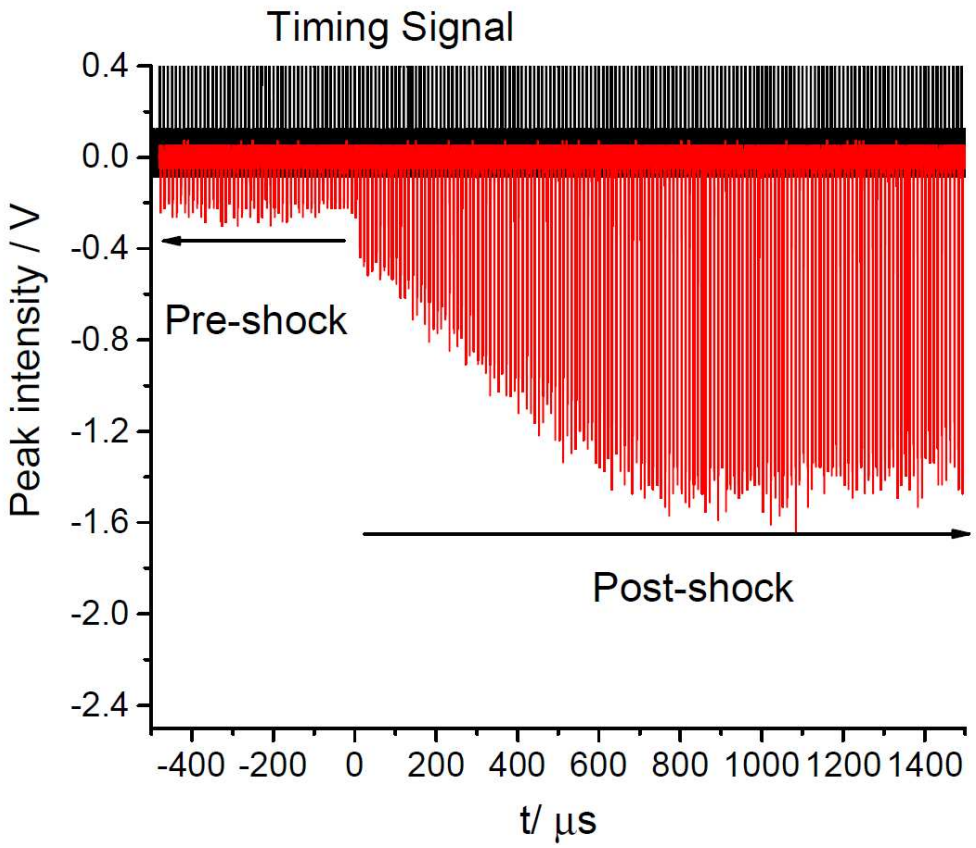

Figure 2: Raw ST/TOF-MS data obtained at a repetition rate of 100 kHz. The experimental conditions are p_5 = 825 Torr, T_5 = 990 K, mixture composition of 5.06% Ar/1.25% $C_3H_6O_3$/93.69% Ne.

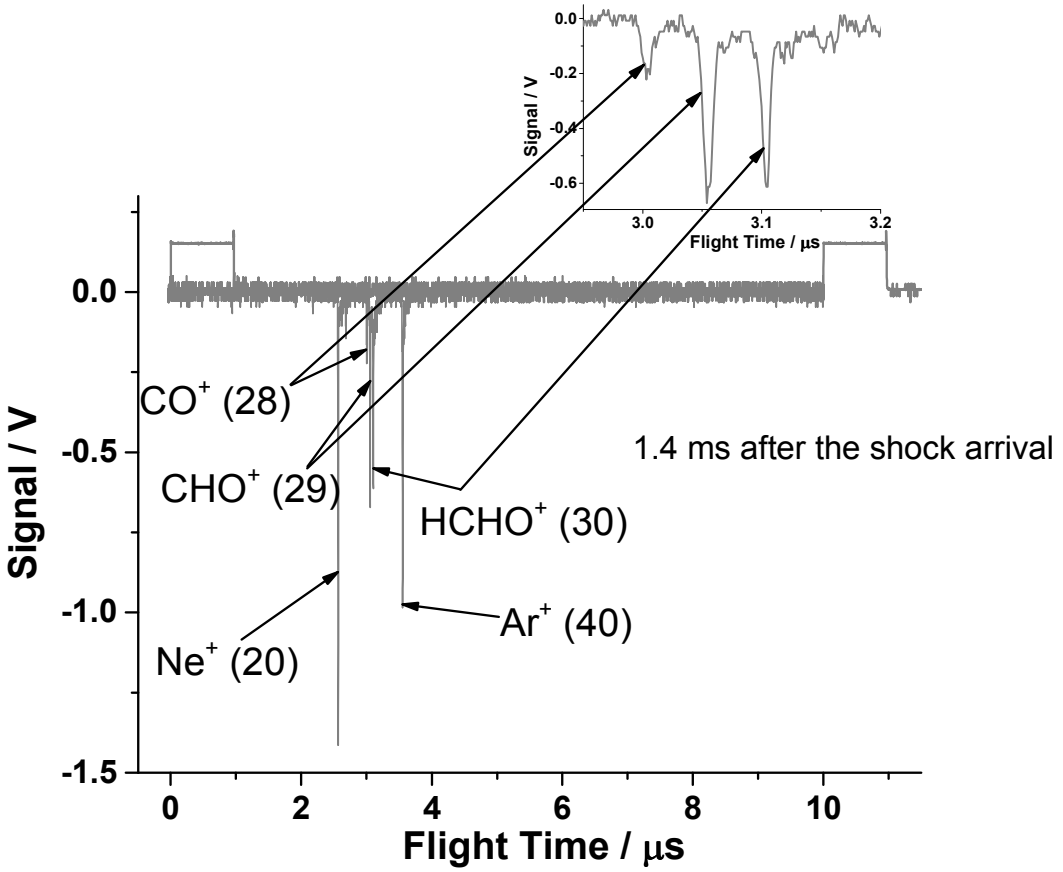

Figure 3: A 10 μs time segment, after 1.4 ms of reaction time, showing the reaction products of 1,3,5-trioxane dissociation. The mass spectrum shows the fragments of formaldehyde. Ions are identified by their *m*/*z* values in the parentheses. Experimental conditions: p_5 = 900 Torr, T_5 = 1082 K, mixture composition of 3.49% Ar/1.58% $C_3H_6O_3$ /94.93% Ne. The inset figure shows an excellent separation of masses differing by *m*/*z* = 1.

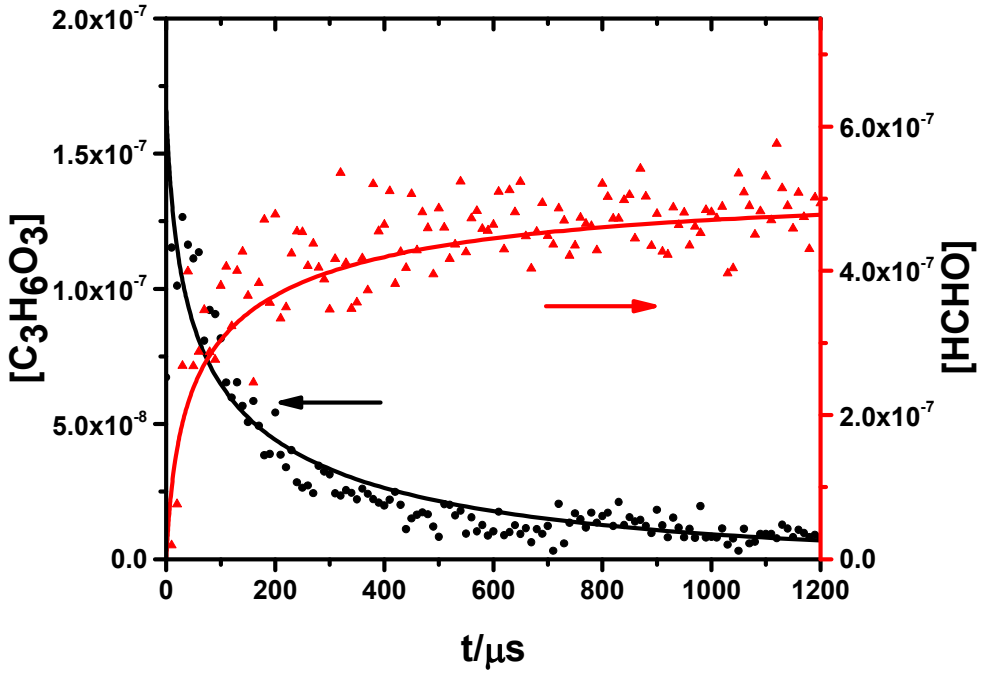

Figure 4: Concentration-time-profiles for 1,3,5-trioxane ($C_3H_6O_3$) and formaldehyde (HCHO). Experimental conditions are p_5 = 818 Torr, T_5 = 990 K, mixture composition of [Ar] = 6.70×10^{-7} mol/cm^3, [$C_3H_6O_3$] = 1.66×10^{-7} mol/cm^3, [Ne] = 1.24×10^{-5} mol/cm^3. Solid lines are the best fit of kinetic simulation.

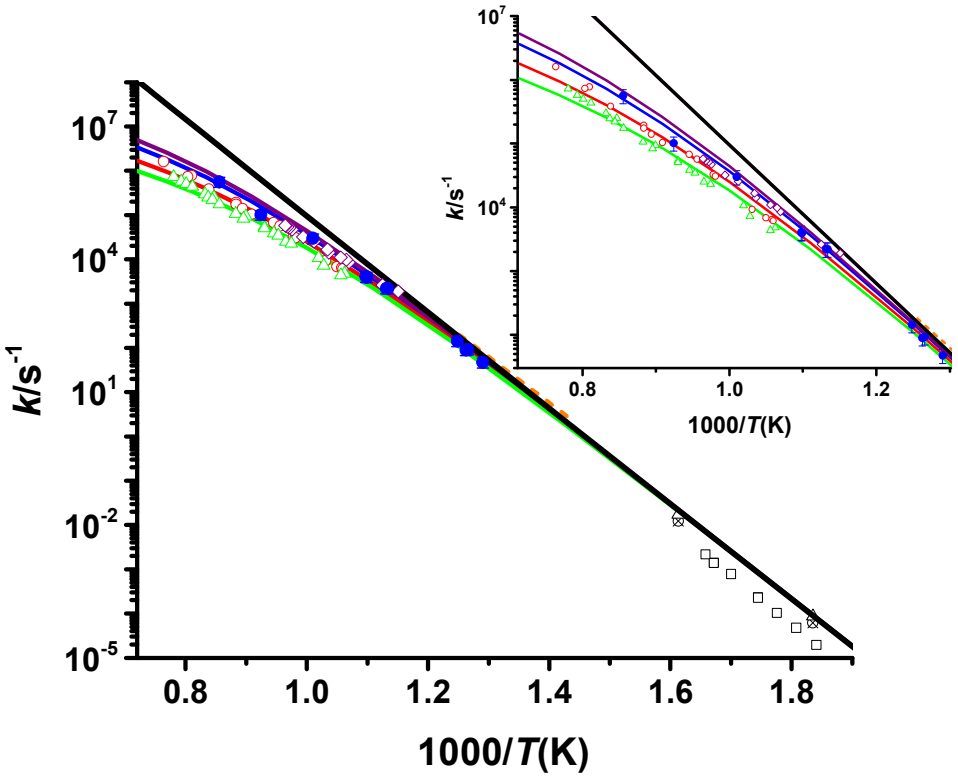

Figure 5: Comparison of the calculated rate coefficients with the experimental data. (●) this work at ≈ 900 Torr, (o) 290-362 Torr [14]; (Δ) 138 -178 Torr [14]; (Δ) 20 – 80 Torr [11]; (⊗) ≤ 100 Torr [15]; (---) 760 Torr [13]; (□) 800 Torr [12]; (◊) 1596 Torr [16]; lines represent our RRKM calculations at pressures (*p*) = ∞ (black), 1596 (purple), 900 (blue), 326 (red), 158 (green) Torr (1596 Torr, 326 and 158 Torr were chosen for calculations as these are the mean pressures for Wang et al. [16] and Irdam and Kiefer [14] experiments, respectively). The inset figure highlights the match between the theory and experiments at higher temperatures.

Table 1: Experimental values of the rate coefficients extracted via kinetic simulation of the measured concentration time-profiles of trioxane and formaldehyde.

	T_5 (K)	P_5 (Torr)	[Ar] (mol/cm^3)	[$C_3H_6O_3$] (mol/cm^3)	[Ne] (mol/cm^3)	k (s^{-1})
1	775 ± 6	908	4.65×10^{-7}	2.16×10^{-7}	1.81×10^{-5}	47
2	790 ± 3	930	6.85×10^{-7}	2.15×10^{-7}	1.80×10^{-5}	92
3	792 ± 3	863	8.10×10^{-7}	2.00×10^{-7}	1.65×10^{-5}	89
4	801 ± 5	818	5.84×10^{-7}	1.88×10^{-7}	1.56×10^{-5}	143
5	882 ± 3	885	6.07×10^{-7}	1.84×10^{-7}	1.52×10^{-5}	2200
6	884 ± 5	810	6.44×10^{-7}	1.80×10^{-7}	1.39×10^{-5}	2199
7	910 ± 4	1065	5.05×10^{-7}	2.25×10^{-7}	1.80×10^{-5}	3933
8	911 ± 5	1073	9.00×10^{-7}	2.42×10^{-7}	1.77×10^{-5}	4053
9	990 ± 6	818	6.70×10^{-7}	1.66×10^{-7}	1.24×10^{-5}	29906
10	1082 ± 6	900	4.66×10^{-7}	2.11×10^{-7}	1.27×10^{-5}	101509

Table 2: Rotational constants (*A*, *B*, and *C*) and harmonic frequencies (ν_i) of the stationary points calculated at the MP2/aug-cc-pVDZ level of theory. Frequencies are scaled by 0.9615.

Species	A, B, C (cm^{-1})	ν_i (cm^{-1})
1,3,5-Trioxane	0.173748 0.173748 0.096858	293, 293, 462, 501, 501, 714, 913, 913, 928, 940, 1031,1031, 1137, 1137, 1187,1194, 1272, 1272, 1333, 1368, 1368, 1436, 1436, 1457, 2877, 2877, 2887, 3082, 3082, 3085
TS	0.141732 0.141732 0.078780	515*i*, 201, 202, 274, 274, 344, 434, 434, 487, 837, 876, 876, 1082, 1174, 1174, 1186, 1186, 1193, 1366, 1400, 1400, 1519, 1555, 1555, 2886, 2887, 2887, 3042, 3042, 3043
CH_2O	9.333951 1.261052 1.110958	1142, 1204, 1468, 1661, 2863, 2944
Barrier (E_0)	46.5 kcal/mol	
Collision Parameters: $C_3H_6O_3$ Ne $\langle\Delta E\rangle_{down}$	 σ = 6.042 Å; ε/k = 533 K σ = 2.82 Å, ε/k = 32 K 500 cm^{-1}	

Table 3: The parameters obtained from the fit[a] of the calculated values for the pressure dependent rate coefficient over the temperature range of 500 to 1400 K.

[a] $k(T) = A\ T^n \exp(-E_a/RT)$ in the units of cm^3, mol, s, cal and K.

	P (Torr)	*A*	*n*	E_a
1	0	8.49×10^{81}	-19.05	60528
2	10	7.76×10^{77}	-19.65	70347
3	100	3.45×10^{71}	-17.40	69660
4	158	2.85×10^{69}	-16.72	69135
5	326	4.23×10^{65}	-15.48	68035
6	760	2.70×10^{60}	-13.82	66376
7	900	2.08×10^{59}	-13.47	66002
8	1596	2.51×10^{55}	-12.24	64651
9	7600	1.56×10^{44}	-8.74	60555
10	76000	2.15×10^{29}	-4.16	54785
11	∞	6.85×10^{15}	0	49537

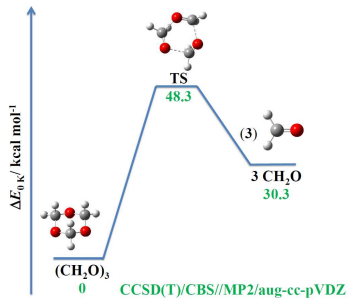
TS
48.3
(3)
3 CH2O
30.3
(CH2O)3
0
CCSD(T)/CBS//MP2/aug-cc-pVDZ
ΔE0 K / kcal mol-1

TOC Graphic